fMRI Activation in Human Visual Cortex Measured with Steady State Free Precession at 3 Tesla

K. Zhong[1], J. Leupold[1], J. Hennig[1], O. Speck[1]

[1]Dept. of Diagnostic Radiology, Medical Physics, University Hospital Freiburg, Freiburg, Germany

Introduction: Recently, increased interest arises in balanced steady-state free precession (bSSFP) techniques to measure neuro-functional activation (1-4). Due to the frequency response profile, the SSFP signal intensity is sensitive to frequency shifts, e.g. in and around blood vessels due to increased oxygenation following neuronal activation, which is typically on the order of 5 Hz. Studies using such methods were performed at 1.5 T and reported functional activation from 5% up to more than 10% in the human visual cortex. This is larger than that from EPI measurements, which is typically 2~3%. One recent study at 4 T used on-resonance conditions for bSSFP measurements and also observed strong activation compared to EPI acquisition. However, there are up-to-date no studies that fully investigated the SSFP contrast mechanism during neuronal activation. This paper analyzes the SSFP signal and contrast behavior at 3 T in fMRI, using a fully balanced multi-echo SSFP sequence. Measurements with a wide range of TR/TE values were acquired and the SSFP spin evolution properties are extracted from the signal. The fMRI activations obtained at different TR/TE times were evaluated, compared to numerical simulations, and the contrast mechanism is discussed. Finally, the contrast-to-noise ratio (CNR) of SSFP was determined and compared to that of EPI methods.

Theory: The steady state SSFP transverse magnetization, without considering diffusion effects, was described previously by Scheffler et al. (5). In essence, we have extended this theory to show that the SSFP transverse magnetization after excitation is given by: $M_{xy}^{+}(\tau) = M_0 \cdot \frac{TR}{T_1} \cdot \sin\alpha \cdot \exp(\tau / T_2') \cdot \Psi(\tau)$, where $\Psi(\tau) = \left| \int_V p(\theta) \left(\frac{1 - E_2 \cos\theta + i\, E_2 \sin\theta}{D} \right) \exp(i\theta\tau / TR)\, d\theta \right|$ is defined as the SSFP dephasing coefficient. θ is the phase evolution during TR, and $p(\theta)$ is the dephasing distribution within the imaging volume V. $E_{1,2} = \exp(-TR/T_{1,2})$ and $D = (1 - E_1 \cdot \cos\alpha)(1 - E_2 \cdot \cos\theta) - E_2 \cdot (E_1 - \cos\alpha)(E_2 - \cos\theta)$. Thus, the SSFP steady state signal increases with TR/T_1, $\Psi(\tau)$ and decays exponentially with T_2' which takes a value between T_2 and T_2* and decreases with increased TR. It will be shown later that the spin echo approximation for SSFP (5) breaks down for TR ≅ T_2*, and therefore the signal follows a modified T_2 decay, e.g. T_2' instead of T_2 proposed originally (5). Simulations were performed in order to understand the SSFP signal behavior at longer TRs, especially regarding the intra-voxel spin dephasing effects arising from $\Psi(\tau)$. A two-compartment model was used, which assigned each voxel a gray matter content and a blood pool. The blood volume was set between 5-10% to account for tissue heterogeneity and randomization of intra-voxel dephasing was used to simulate in vivo field inhomogeneity effects. T_1 and T_2 values for tissue and blood at 3T were taken from the literature. Simulated signals were estimated by intra-voxel based complex averaging followed by magnitude summation of signals from all voxel in an ROI. A T_2 change of 5 ms was used to calculate the activated signal. The simulation results suggest an exponential decay of the signal and an increase of activation with TE, and are compared with measured data in the discussion.

Methods: All experiments were performed on a 3 T whole-body scanner (Siemens, Erlangen, Germany) with the standard 8-channel head coil. Six volunteers (aged between 25 and 37 years) participated in the study. A block design (ON/OFF time 20/20 s, 3 blocks) using a circular checkerboard stimulus inverting at 8 Hz was presented. Subjects were instructed to fixate at all time on a red fixation cross centered in the checkerboard. An active color change task was assigned to keep the subject's attention on the stimulus throughout the measurement. Axial TSE images parallel to the calcarine sulcus were obtained and a slice which exposed large parts of the visual cortex was chosen for subsequent functional imaging. fMRI acquisitions started with gradient echo EPI (Flip angle = 90°, TR/TE = 500/30 ms, FOV = 22 x 22 cm^2, 64 x 64 matrix, 3 mm slice thickness), followed by repeated measurements with multi-echo bSSFP (Figure 1; flip angle = 60°, 64 x 64 matrix; on-resonance condition) in the same slice at five different TR and multiple TE conditions. The acquisition order of the five TR conditions was randomized for each subject. Data analysis used routines written in MATLAB (The Mathworks, Natick, USA). SPM2 (University College London, UK) was used for fMRI analysis. EPI data were used to determine the activated area in the visual cortex, and a mask was generated from the statistic map ($p < 0.001$). This mask was subsequently applied to all multi-echo SSFP data to calculate the time course in the activated region as the averaged signals.

Results and Discussion: EPI activation is 4.2 ± 0.45% and is consistent within the group. This suggests that the checkerboard stimulus used in the current study with an active task can produce very stable and reproducible results. SSFP acquisition (TR/TE = 6.5/3.2 ms) shows activation of 2.4 ± 0.33% and is also quite reproducible. Signal decay vs. TE is shown in Fig. 2 for different TRs (15 – 70 ms). The common spin echo behavior with a signal maximum at TR/2 is not observed, which suggests that the spin-echo assumption (5) is not valid for this TR range at 3 T. Exponential fitting of the signal decay for different TR results in an apparent T_2', which changes from 60 to 35 ms. A T_2'—TR L-curve has a converge point around TR =30 ~ 40 ms. This correspond to the typical T_2^* value in the occipital lobe. Therefore, one can postulate that TR ≅ T_2* is the condition where SSFP starts to behave more like a gradient echo due to the averaging process over different off-resonance frequencies. The measured activation changes are shown in Fig. 3, together with the regression fit (red) and the simulated activation (blue). The simulated activation fits well the measured data, with a small difference in activation level. This is probably affected by the choice of parameters in simulation. Regression fit has a different slope compare to simulation. This may be due to the fact that the simulated curve uses T_2 while the actual signal depends on T_2'. The overall agreement between simulated activation and measured data suggests that the SSFP contrast can be explained by the standard BOLD mechanism. The activation CNR is shown in Fig. 4. The TE curve for TR = 70 ms resembles quite closely the gradient echo BOLD vs. TE response, which confirms our postulation that SSFP shows a behavior similar to gradient-echo. The overall SSFP CNR remains lower compared to EPI. This is due to a small SSFP steady-state magnetization (T_2/T_1) in the brain.

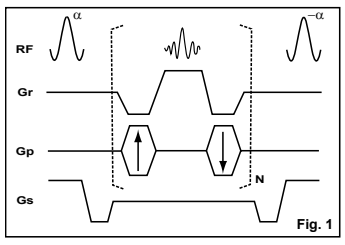

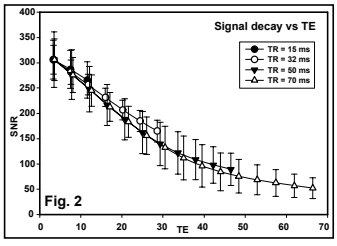

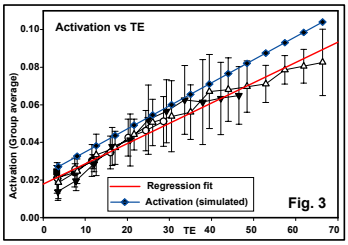

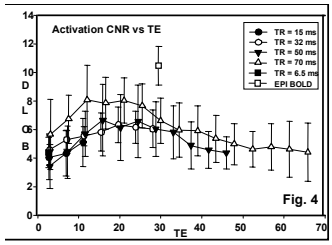

Fig. 1: The multi-echo bSSFP sequence diagram (4.2 ms echo spacing); Fig. 2: Signal decay vs TE for different TR (normalized); Fig. 3: Relative activation vs TE for different TRs. Regression fit (red) simulated activation (blue); Fig. 4: Activation CNR comparison, including EPI. Group averaged results are reported.

Conclusion: This study investigated the SSFP fMRI contrast at 3 T at various TR and TE. The contrast can be explained by a BOLD mechanism. SSFP shows a behavior similar to gradient echo at moderate TRs. The relative SSFP activation at longer TR/TE is higher than EPI. However, SSFP CNR is lower compared to EPI.

Reference:

1. Scheffler K, et al. NMR Biomed 2001;14(7-8):490-496.
2. Dubois J, et al. Proc Intl Soc Mag Reson Med 2002:117.
3. Miller KL, et al. Magn Reson Med 2003;50(4):675-683.
4. Bowen CV,et al. Proc Intl Soc Mag Reson Med 2005;13:119.
5. Scheffler K. et al. Magn Reson Med 2003;49(2):395-397.